Pollution 2022, 8(1): 281-293
DOI: 10.22059/POLL.2021.323942.1090

RESEARCH PAPER

Evaluation of Efficiency of Iron Oxide Nanoparticles (Fe_3O_4@CNT) in Removal of Malathion in Aqueous Medium Using Response Surface Methodology (RSM)

Malektaj Eskandari makvand, Sima Sabzalipour*, Mahboobeh Cheraghi and Neda Orak

Department of Environment, Ahvaz Branch, Islamic Azad University, Ahvaz, Iran.

Received: 16.05.2021, Revised: 28.10.2021, Accepted: 24.11.2021

ABSTRACT
Organophosphates are one of the most common pesticides in the world. Among them, one can find malathion that is classified as carcinogenesis, and, as a result, should be appropriately removed since it is highly consumed and possesses a lot of pathogenicity. So far, several processes have been used to remove malathion from aqueous media. The present study investigates its removal by means of Fe_3O_4 iron oxide nanoparticles. Based on experimental-laboratory studies, using the Response Surface Methodology (RSM), the impact of independent variables such as pH, iron oxide nanoparticle concentration, and contact time on malathion removal efficiency have been investigated. Results show that the pH of the solution is the most important and effective parameter in the process. Optimal conditions of malathion removal based on the appropriate model, obtained from RSM, include 0.4 g/L iron oxide nanoparticles, pH of about 5 (acidic conditions), and contact time of about 1 h with ultraviolet radiation being equal to 82% malathion removal. The process, used in this study, can remove malathion from aqueous solutions according to the so-called conditions, and changing the laboratory conditions can effectively remove it. This process can also be recommended as an economic and scientific method to remove malathion from drinking water.
Keywords: Modeling, Iron oxide nanoparticles, Malathion, Environment

INTRODUCTION

In recent years, industrial growth, population growth, depletion of water resources, the indiscriminate use of hazardous chemicals in various sectors, and the strengthening of environmental protection laws have led studies to present more effective removal systems (Gajda-Meissner et al., 2020). Most pollutants dissolve in water and enter the environment rapidly and threaten human health. The World Health Organization has identified malathion as a dangerous pollutant (Ch and Jadhav, 2021). Organophosphate pesticides are among the most common pesticides in the world (Prosposito et al. 2020). Unfortunately, the excessive use of organophosphate pesticides in many parts of the world has increased their amount in the environment and has brought about its damage (Surendra et al., 2020). These pesticides can enter water sources in various ways, such as industrial wastewater, agricultural runoff, and the use of chemicals (Abdelhameed et al., 2021). Organophosphate insecticides have allocated about

* Corresponding author Email: Shadi582@yahoo.com

70% of insecticide consumption in the United States and about 40% of insecticide consumption in the world; among them, malathion with the highest consumption, i.e., about 32-34% of the total consumption of organophosphates, has a significant share among insecticides (Aghoutane et al., 2020).

Malathion, with a chemical formula of $C_{10}H_{19}O_6PS_2$, is one of the most dangerous organophosphates toxin widely used and is easily available in our country (Khan et al., 2019a). Mortality from this toxin is due to inhibition and dysfunction of the acetylcholinesterase enzyme, an important enzyme for the functioning of the nervous system (Khan et al., 2019b). So removing these pollutants from water resources is currently considered one of the important issues (Kassiri et al. 2021). Unfortunately, removing this compound has become a significant challenge due to its considerable stability and solubility in water and resistance to traditional removal methods. An ideal treatment method for water and wastewater involves decomposing all available toxic substances without using hazardous substances from the treatment process (Jaafarzadeh et al., 2017).

So far, different combinations and methods have been used to remove or destroy this pollutant. Among them, the use of photocatalytic methods due to high efficiency, the use of free solar radiation, and the prevention of the production of hazardous by-products have attracted a lot of attention (Zhu et al., 2020; Zhang et al., 2017). Numerous reports have been presented on the study of photocatalytic properties of iron oxide (Lin et al., 2021; Ch et al., 2020). However, some shortcomings still limit the widespread use of this class of metal oxides. High clumping, large bandgap (that can only absorb ultraviolet radiation that contains less than 5% of solar radiation), and low surface area are defects that need to be addressed (Nogueira et al., 2020).

The advanced oxidation process has received much attention in recent years, especially advanced photochemical oxidation to remove organic matter in the aquatic environment (Buchman et al., 2020). In this process, organic matter is converted into low-risk materials and, generally, minerals with the combined activity of the oxidizing agent, catalyst, and radiation. The basis of this process is the production of hydroxyl radicals (Zuo et al., 2019). The generated hydroxyl radicals have very high oxidation power and very low selectivity (Olaniran et al., 2017). Thus, by producing hydroxyl radicals under environmental conditions, a wide range of toxic organic matters, even biodegradable organic matter, is converted to harmless substances such as carbon dioxide and water, so less toxic and more biodegradable materials are produced (Hong et al., 2020). In the process of catalytic oxidation, biomaterial destruction (malathion) occurs due to the combined activity of three oxidizing agents, a high-energy radiation source and a semiconductor optical catalyst (Sagir et al., 2021). The oxidizing agent is generally the optical catalyst of semiconductors of metal oxides, especially titanium dioxide (TiO_2), zinc oxide (ZnO), and trivalent iron oxide (Fe_3O_4) (Bacchetta et al., 2017). The oxidation process is also better accomplished by ultraviolet radiation, which activates the catalyst and produces free hydroxyl radicals (Mehdipour et al., 2020). The filtration of nanoparticles leads to a change in the energy gap and precision engineering, and stoichiometric addition of energy gap metal oxides can be reduced, and a shift in required activation energy from ultraviolet to visible radiation can be created (Bozich et al., 2017). One of the design concepts of tests is Response Surface Method (RSM). RSM is a set of mathematical equations and statistical techniques for optimizing the adsorption process and can simultaneously examine the importance of several factors influencing the adsorption process.

The RSM method was first introduced in 1959 by Box and Wilson (Yazdani et al., 2014). This method can consider the interactions between parameters and provide a mathematical model for predicting process responses. Other advantages include finding the optimal point

outside the tested points with an accuracy equal to the tested points and providing two-dimensional and three-dimensional diagrams. RSM is a useful technique for evaluating several input variables that affect performance scales or quality characteristics of the product or process under evaluation (Titus et al., 2019). This method is also a useful tool in optimizing parameters. This present study sought to determine the decomposition efficiency of malathion using iron oxide nanoparticles (Fe_3O_4) by RSM.

MATERIALS AND METHOD

This study was an experimental-laboratory study that used iron oxide nanoparticles (Fe_3O_4) to remove malathion in aqueous media as a catalyst in the photocatalytic process. Malathion with 98% purity and persulfate salt was prepared from the German Merck factory. To synthesize magnetic iron oxide nanoparticles (Fe_3O_4), first 0.1 g of vitamin C was mixed with two solutions of iron chloride (quaternary divalent iron chloride $FeCl_2$). $FeCl_2(4H_2O)$ and hexavalent trivalent iron chloride $FeCl_3(6H_2O)$) in a ratio of 1: 2. Vitamin C inhibited the oxidation of divalent iron during the reaction, and the resulting solution was stirred for 10 to 15 min. The pH of the solution was then raised to 10 using ammonia solution. The resulting solution was then placed at 80 °C for 30 to 40 min. The following reaction carried out to synthesize Fe3O4 nanoparticles

$$Fe^{2+} + 2Fe^{3+} + 8OH^- \longrightarrow Fe_3O_4 + 4H_2O$$

Finally, the resulting precipitates were washed with distilled water and ethanol and placed in an oven at 60 °C for 10 h and dried. Finally, Fe_3O_4@CNT nanocomposite with a concentration of 1 to 25.6×10^{-2} g/l was obtained. X-ray diffraction (XRD) apparatus was used to determine the X-ray diffraction pattern and the presence of Fe and Magnetite particles in the catalyst structure. EDX analysis was used to determine the ratio of elements in the catalyst structure. The surface and morphological characteristics of the catalyst were also investigated using SEM analysis.

The RSM was used to design the adsorbent experiments using the Expert-Design software version 7. The central composite design (CCD), one of the standard RSM methods, was used to investigate effective pH factors, the amount of iron oxide nanoparticles (as catalyst or amount of adsorbent), and malathion concentration, and contact time. This model helps to describe the impact of effective factors and the interaction between them with the least number of experimental runs by obtaining optimal values for each of the influencing factors. All chemicals used in this experiment were ionized in water and then used. The study of the malathion adsorption process in a batch adsorption system was performed in a chamber with a 50 mm solution of malathion at room temperature (27.5 °C). For this purpose, a stock standard solution with a 250 mg/l was made in a volumetric flask. Concentrations of 10, 35, 60, 85, and 110 mg/l were prepared by diluting them. All adsorption experiments were performed by adding a certain amount of iron oxide nanoparticles. For this purpose, five amounts of iron oxide nanoparticles, including 0.3, 0.40, 0.80, 1.05, and 1.3 g/l, were considered.

The pH of the samples was measured before each experiment. Sodium hydroxide (NaOH) and hydrochloric acid (HCl) 0.1 N were used to adjust the pH. The experiment was performed at five pHs of 3, 5, 7, 9, and 11.

RESULTS AND DISCUSSION

SEM test was performed on these particles to determine the structural characteristics of nano-

particles. Figure 1 shows the results of this analysis. The morphology and porosity of the internal structure of MNP have been shown using scanning electron microscopy (FESEM) (Figure 1). Figure 2 shows the FTIR infrared spectroscopy analysis of MNP iron oxide nanoparticles. The observed peaks belonged to the O-Fe group and were compatible with Fe_3O_4 synthesis. Figure 3 shows the XRD pattern of synthesized nano iron oxide to determine the crystalline phase. As can be seen, all the peaks obtained can characterize the phase of pure iron oxide from iron oxide. No impurities were observed according to the XRD pattern. The average crystal size (D) for MNP was calculated according to the Deby-Scherrer equation, $D = 0.99\ \lambda / \beta \cos(\theta)$. In this equation, λ is equal to X-ray wavelength; β is 1.540598Å that expresses the entire full width of the half-maximum scattering line in terms of radians, and θ represents the diffraction angle of the XRD spectrum. The average crystal size of MNP was about 40 nm, which confirms the results obtained from SEM scanning electron microscopy analysis.

The FTIR spectrum shows the nanocomposite. As can be seen, many vibrations are seen, but two strong vibrations occur at 570 and 650, which could be due to the Fe-o bands in the magnetized nanocomposite Fe_3O_4@CNT, respectively. The results of various analyzes to determine the characteristics of nanocomposites showed that nanoparticles synthesized in the range of nanoparticles, mesoporous, with very high magnetic properties and very high purity. FTIR infrared spectroscopic analysis shows MNP magnetite nanoparticles visible peaks belonging to the Fe-o group and compatible with Fe_3O_4 synthesis. The XRD spectrum shows that all peaks obtained can determine the phase of pure magnetite from iron oxide. 16 peaks have been identified which have been favorable results compared to global data. All of the above is to prove the function of magnetite nanoparticles loaded on carbon, which in total has created a favorable structure and mesoporous and with a suitable capacity to remove malathion.

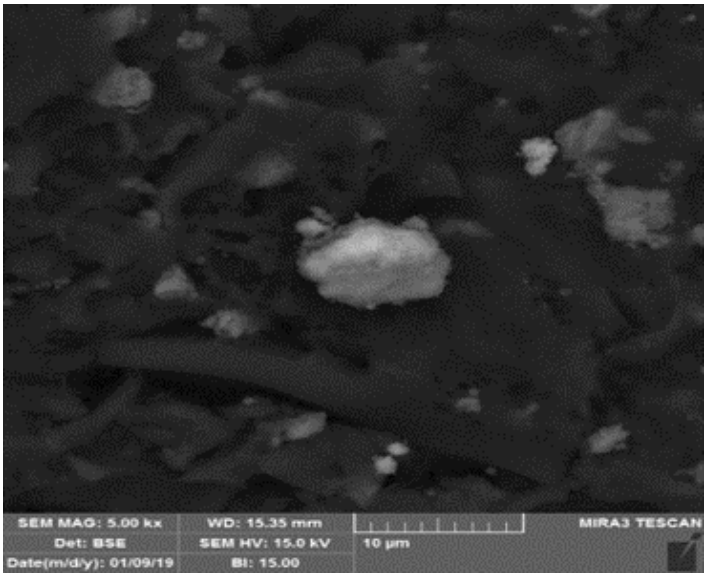

Fig 1. Appearance and properties of ferrite nanoparticles of MNP.

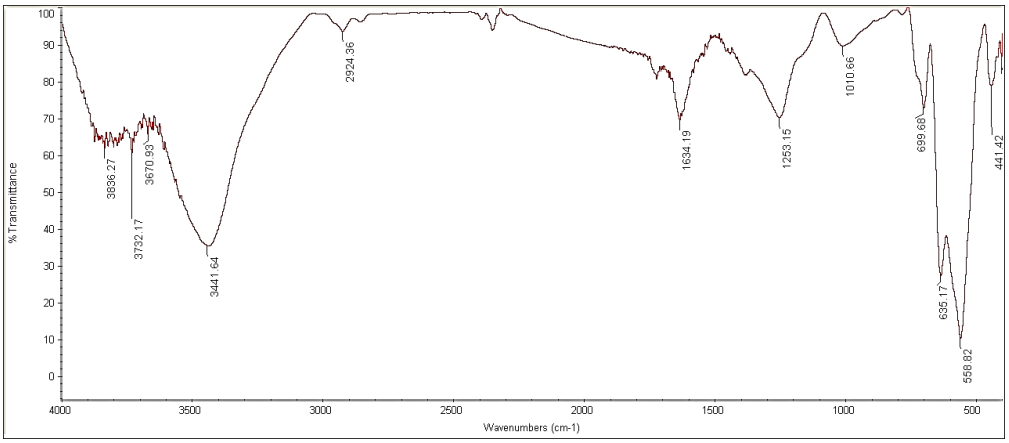

Fig 2. FTIR spectroscopic analysis.

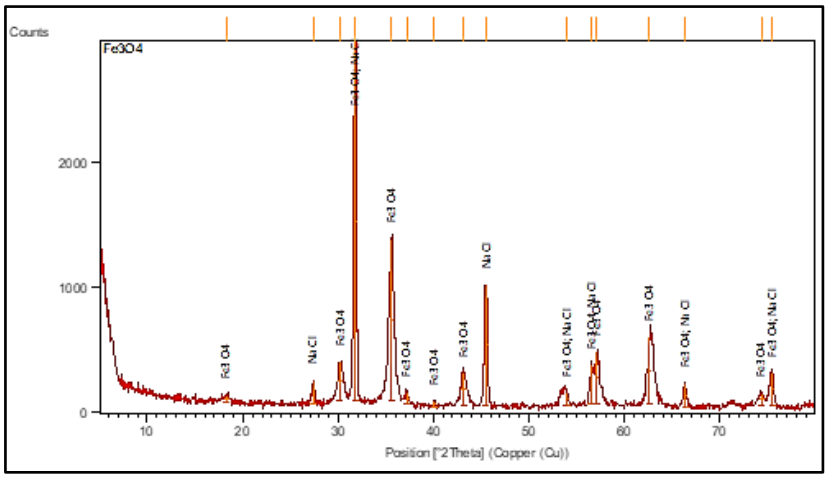

Fig 3. XRD spectrum of synthesized nanomagnet to determine the crystalline phase.

According to the design of the experiment, the results of performed experiments for removing malathion from aqueous media based on the nano photocatalytic method are given in Table 1. The results of designed Run tests for removing malathion were analyzed using CCD and four regression models by Expert-Design software (Table 2); the statistical results for each model are given. The quadratic model was approved as the optimal regression model to confirm the experimental Run designed among the models, considering that it has the lowest standard deviation (0.088) and the highest determination coefficient of R^2 (0.9785) (justified R^2 is 0.9585 and predicted R^2 is 0.8789).

Table 1. Results of experiments designed using CCD method.

Malathion removal percentage	Contact time (min)	pH	Malathion concentration (mg/l)	Nano particle value (g/l)	Experiment Run
21.7	50	9	35	1.05	1
23	100	9	35	0.55	2
64.5	100	5	85	1.05	3
71.33	125	3	35	1.05	4
74	100	7	60	0.3	5
17	100	9	85	0.55	6
82	60	5	35	0.40	7
57.7	25	5	110	1.3	8
3.4	75	11	60	0.80	9
72	50	7	100	0.80	10

Table 2. Proposed models by Expert-Design software.

The sum of the squares of the predicted residual values	Predicted R^2 determination coefficient	R^2 adjusted determination coefficient	Determination coefficient R2	Standard deviation	Reference
1.04	0.8073	0.8546	0.8747	0.16	Linear
1.36	0.7482	0.8147	0.8786	0.19	Interaction effect
0.65	0.8789	0.9585	0.9785	0.088	Quadratic effect
7.58	-0.4051	0.9571	0.9896	0.089	Cubic effect

The quadratic regression equation, which shows the experimental relationship between the experimental variables and the coded malathion removal efficiency, was obtained.

(Removal)0.26 = 2.52147 + 1.72529 (Dosage Amount) - 4.38768E - 003 (Nitrate Concentration) + 0.16225 (pH) - 8.40945E - 003 (Time) - 1.02534 (Dosage Amount)2 - 0/026580(pH)2 + 7.96720E - 005 (Time)2

Results of analysis of variance (Table 3) obtained from the quadratic model for malathion removal using the nano photocatalytic method show that the parameters of contact time, malathion concentration, pH, and to a lesser extent, nanoparticles had a significant effect on the model. The P-values for most of the factors studied in the quadratic regression model are less than 0.05 and have a significance level of 95%. This represents a high degree of significance for the quadratic model and confirms its suitability for the performed experiments. Also, the value of the F-value for the model is 95.109; its high value shows the significance of the model. Also, the fitting and significance of the model were evaluated through the R^2 determination coefficient and the adjusted R^2 determination coefficient. The very high value of the determination coefficient R^2 of 0.9722 and the adjusted determination coefficient R^2 of 0.9634 indicates the high significance of the model and the very high ability of the proposed model to predict changes. If the number of studied factors is large and the sample size is not large, the adjusted determination coefficient R^2 may be significantly smaller than the determination coefficient R^2; this value is very close to each other in this study. On the other hand, low values of standard deviation (SD = 0.083) and coefficient of variation (CV = 3.25) indicate the high accuracy and low error of experiments.

Table 3. Results of analysis of variance for quadratic mode model.

	The significance level *(p)*	Fischer statistic (F)	Mean of squares	Degree of freedom (DF)	Sum of squares	Reference
Type of determination coefficient R^2	<0.0001	109.95	0.75	7	5.24	Model
determination coefficient R^2	0.2217	1.58	0.011	1	0.011	Nanoparticle value
	<0.0001	42.40	0.29	1	0.29	Malathion concentration
	<0.0001	620.84	4.23	1	4.23	pH
	<0.0001	27.62	0.19	1	0.19	Contact time
Adjusted determination coefficient R^2	0.0005	16.88	0.11	1	0.11	Nanoparticle value
	<0.0001	46.47	0.32	1	0.32	pH
	0.0042	10.19	0.069	1	0.069	Contact time

Interactions of healthy effect parameters of malathion concentration, amount of iron oxide nanoparticles (adsorbent amount), contact time, and pH for removal malathion from aqueous solutions using nano photocatalytic method by three-dimensional diagrams are shown in Figure 4. The optimal values of the parameters were considered according to the performed test runs for malathion removal from aqueous solutions by Expert-Design software and standard RSM method (Table 4). After identifying the individual effects of the parameters on the system response, the interaction effects or dual effects of the factors should be examined. The best way to express interactions is to use 3D diagrams. In these graphs, the considered variable changes, while the rest of the parameters are kept constant.

Table 4. Optimal values for the percentage of malathion removal from aqueous solutions.

Nanoparticle value (g/l)	Malathion concentration (mg/l)	pH	Contact time (min)	Malathion removal percentage	The desirability of optimal values
0.40	35.15	5	60.02	82	0.968

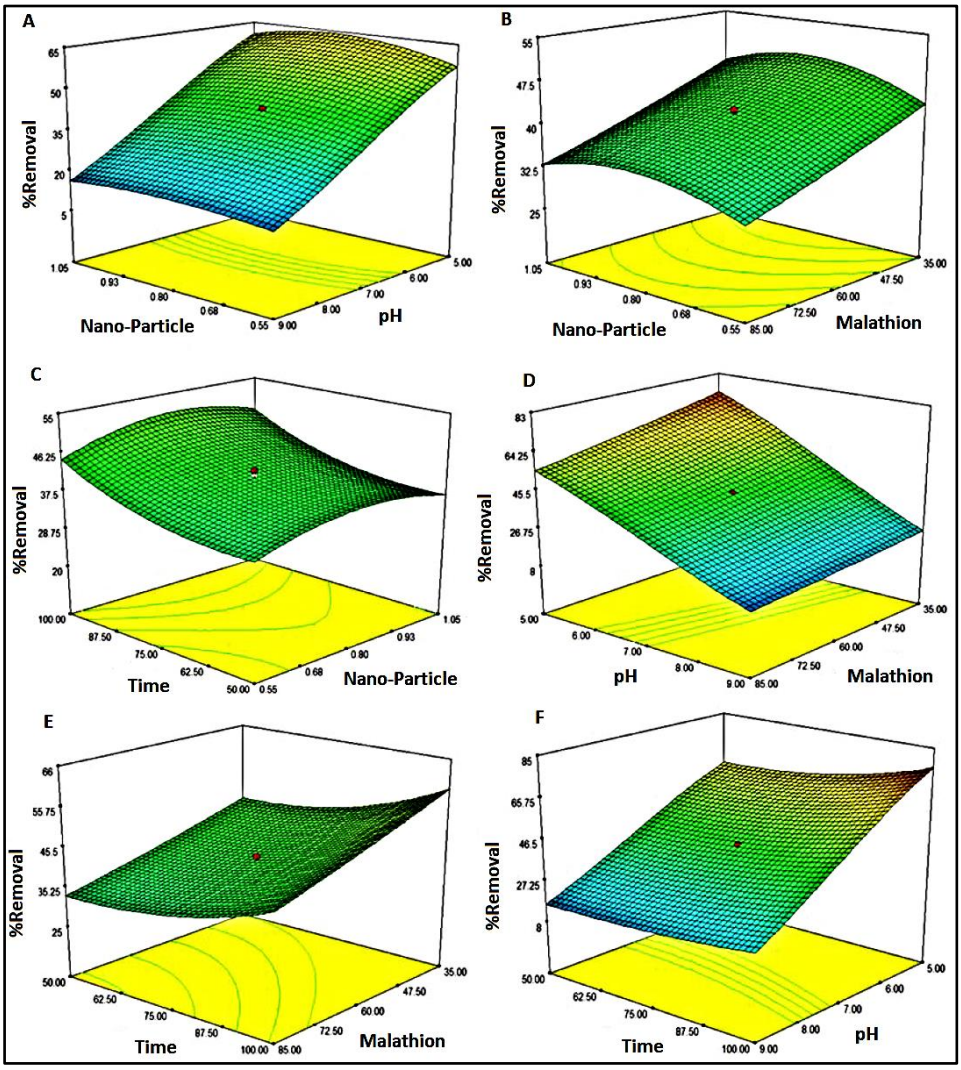

Fig 4. Surface-response: effect of various parameters; A: nanoparticles, B, pH: nanoparticles and malathion, C: time and nanoparticles, D: pH and malathion, E: time and malathion, F: time and pH.

In this study, the effect of pH in the range of 3 to 11 in the presence of iron oxide nanoparticles of 0.1 g/l at a reaction time of 60 min was investigated, and their optimal values were

determined by RSM (Figure 4). The RSM method is widely used in many research fields today for designing experiments and providing logical relationships between variables. Experimental methods and statistical analysis of the model showed that the value of R^2 = 0.9722, indicating that this model is defines the removal of malathion by photocatalytic process (Fe_3O_4) defines the removal of malathion by photocatalytic process (Fe_3O_4) defines the removal of malathion by photocatalytic process (Fe_3O_4). However, the value of the adjusted determination coefficient R^2 of 0.9634 is less than the value of the determination coefficient R^2. The optimum point for malathion removal efficiency of 82% is achieved at a dose of 0.4 mg/L iron oxide nanoparticles, an initial malathion concentration of 23 mg/L, a pH of about 5, and the reaction time of 1 h.

Figure 4.A shows a three-dimensional diagram of malathion removal efficiency as a pH and iron oxide nanoparticle concentration function. It is observed that malathion removal efficiency is increasing rapidly with decreasing pH and increasing iron oxide nanoparticles. The removal process at a pH of about 5 is faster. As the results show, the highest removal is done at acidic pHs, while the removal efficiency decreases at alkaline pHs. Figure 4.B shows a three-dimensional diagram of the interaction of iron oxide nanoparticles and malathion on the removal efficiency. According to this diagram, nanoparticles' concentrations of more than 1.05 mg/l increase the removal efficiency. Figure 4.C shows a three-dimensional diagram of removal efficiency. It is observed that with increasing time and concentration of nanoparticles, the percentage of malathion removal increases. Figure 4-D shows a three-dimensional diagram of removal efficiency. As can be seen, decreasing the pH (acidic) increases the malathion removal. Figure 4.E shows a three-dimensional diagram of the interaction of time and malathion in the removal efficiency. With increasing time, the concentration of malathion decreases, and the removal process occurs more rapidly. Figure 4.F shows a three-dimensional diagram of the effect of time and pH; it can be concluded that with increasing time and decreasing pH, the removal of malathion increases.

Contact time is one of the effective parameters in increasing the performance of photocatalytic systems. Malathion was placed at a photocatalytic reactor for 25, 50, 60, 75, 100, and 125 min under ultraviolet radiation, and the effect of contact time on the malathion removal process was investigated. The results showed that the percentage of malathion removal from aqueous solutions increased with increasing exposure time to ultraviolet radiation. For example, the removal efficiency increased from 57.7% in 25 min to 82% in 60 min, which is consistent with the study of Qhasemi et al. They found that the removal efficiency of 69% in 30 min reached 80% in 240 min, and the contact time was optimal for the removal of the contaminant (Qasemi et al., 2016). The reason for this can be explained by the decomposition and removal of malathion by free radicals produced, including hydroxyl, due to the electronic excitation of iron oxide nanoparticles during the process (Dehghani Fard et al., 2012). Also, with increasing contact time, due to the increase in the collision probability of malathion with the adsorbent surface (nanoparticles), the surface adsorption increases, and as a result, the percentage of malathion removal increases (Chhingombe et al. 2006). The effect of malathion concentration at concentrations of 35, 60, 85, 100, and 110 mg/l was investigated to remove malathion from aqueous solutions. increasing the initial concentration of malathion, its removal percentage decreased, and the malathion removal efficiency decreased from 82% at 35 mg/l to 57.7% at 110 mg/l. This is consistent with the results of Parastar et al. on the photocatalytic removal of malathion from aqueous solutions using the process of zinc oxide nanoparticles and ultraviolet (UV) radiation. This study was performed at malathion concentrations of 30, 35, 50, 60, 85, 100, and 150 mg/l, and the percentage of malathion removal decreased with increasing initial concentration. Also, one of the reasons for the removal of

malathion at low concentrations is the absorption of some radiation by malathion itself. Thus, malathion acts as an optical filter at wavelengths less than 355 nm (Parastar et al., 2012). Furthermore, large amounts of malathion are adsorbed on iron oxide nanoparticles at higher concentrations, preventing its molecules from reacting with free radicals and electron holes (Ehrampoosh et al., 2010). As the concentration of malathion increases, the optical photon transfers decreases, and the malathion absorbs the optical photons before reaching the iron oxide catalyst particles (Chakrabarti et al., 2004).

Another influential factor in the photocatalytic removal process is. The concentration of catalyst or nanoparticles in the removal process, affecting the removal process by affecting the number of available active sites. The effect of iron oxide on the malathion removal process was investigated in five different concentrations including 0.3, 0.40, 0.80, 1.05, and 1.3 g/l. Initially, by increasing the amount of nanoparticles to 0.3 and 0.40 g/l, the percentage of malathion removal increased by 74 and 82%, respectively, and then increased the amount of nanoparticles by 1.05 and 1.3 g/l the percentage of removal decreased by 21.7% and 34%, respectively. The findings are consistent with the study of Javid et al. on the efficiency of the photocatalytic oxidation process of reactive blue 19 with titanium dioxide nanoparticles and titanium dioxide nanofibers. The highest percentage of pollutants removal was observed at a concentration of 0.4 mg/l (Javid et al., 2015). The reason may be that initially with increasing the concentration of nanoparticles, the number of absorbed photons increases, the number of active and available sites increases, and more malathion molecules are attracted (Parastar et al., 2012). The removal efficiency of malathion in the amounts of 1.05 and 1.3 g/l was less than 0.40 and 0.8 mg/l, respectively. The results are also consistent with the study of Goa et al. on the decomposition of phenol by titanium dioxide nano photocatalyst in wastewater (Guo et al., 2006).

pH is an important factor in the decomposition and removal of organic pollutants by semiconductor oxides (such as iron oxide) by affecting pollutant molecules, catalyst surface charge, rate, and mechanism of hydroxyl radical production (Qhasemi et al., 2016). So, this study was performed at three acidic pHs (pH =3 and 5), neutral (pH = 7), and alkaline (pH = 9 and 1). The results showed that the highest percentages of malathion removal at acidic pH (pH = 5) were higher than neutral and alkaline pH; the efficiency of malathion removal increased from 3.4% at pH =11 to 82% pH= 5. Reasons for the higher removal efficiency of the malathion at acidic pH can be attributed to the fact that the reaction occurred in the solution on the surface of iron oxide. Since negative sites on the photocatalyst surface cannot effectively absorb malathion anions, increasing the pH reduces the percentage of malathion removal (Parastar et al., 2012). The results of this study are consistent with the results of Soares et al. on the photocatalytic reduction of malathion using titanium dioxide in the presence of palladium and copper (Soares et al., 2014).

Alcohols are used to scavenge both hydroxyl radicals and sulfate radicals to determine the active species in the decomposition of pollutants in sulfate radical-based processes. Benzoic acid (BA) was used due to its very high reaction rate with sulfate radical and hydroxyl radical. Its reaction constant for hydroxyl radical and sulfate is 1.4 - 2.2 × 10^9 $M^{-1}S^{-1}$. The reaction rate of this alcohol compared to the sulfate radical is a thousand times lower, so we can find the sulfate radical contribution based on the difference between these two matters. In the presence of BA, the amount of decomposition and removal of malathion decreased significantly to 21%, which indicates the participation of the sulfate and hydroxyl radicals in the decomposition of malathion. The rate of decomposition reached 46% during the 60 min reaction time in the presence of tert-butyl alcohol (TBA), indicating this phenomenon. Hydroxyl radical plays a lesser role than sulfate radical in malathion degradation. In fact, sulfate radical in aqueous

solution can be converted to hydroxyl radical. Similar results have been recorded by Zhou et al. (2015), Nidheesh et al. (2013), and Yao et al. (2014). In general, the results showed that all three active species in this system play an important role in the decomposition of matter, but the degradation of malathion depends on sulfate radicals. Hence, sulfate radicals play a significant role in malathion oxidation based on quenching (Figure 5).

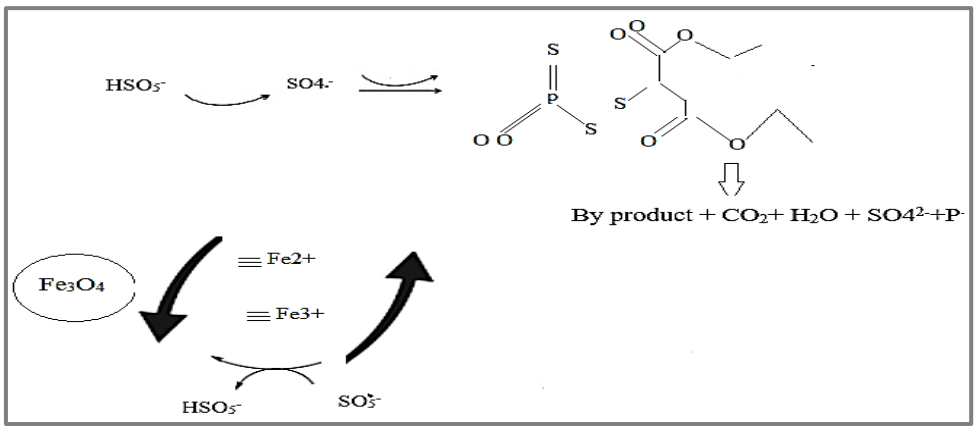

Fig 5. Schematic view of the studied mechanism for malathion degradation.

CONCLUSION

According to the obtained results and statistical analysis results, the use of the photocatalytic process of iron oxide according to the considered conditions can increase the efficiency of malathion removal. Removal of malathion from aqueous media is influenced by UV exposure time, malathion concentration, nanoparticle content, and pH. The highest percentage of malathion removal of 82% was observed at a contact time of about 1 h with ultraviolet radiation irradiation, acidic pH of 5, and 0.4 g/l concentration of iron oxide nanoparticles. The results also indicated that the nanophotocatalytic process could be optimized to remove malathion from aqueous media using RSM in a number of final and optimized experiments. The results are mentioned as following:

- The most important effective parameter in the malathion removal process was the pH parameter and iron oxide nanoparticles (Fe_3O_4).
- Optimal pH conditions were obtained for the malathion removal process at of about 5 (acidic conditions).
- The mechanism of malathion removal was the highest in acidic conditions and decreased with increasing pH to the alkaline range.

Although the present study results are on a laboratory scale, it can be expected that the introduction of high amounts of nanoparticle oxide into aquatic environments can impose harmful effects on aquatic health and aquatic ecosystems. Therefore, the anticipation of measures to reduce and prevent the entry of harmful amounts of nanoparticle oxide into the aquatic environment and the irregular use of nanoparticles in various marine and aquaculture industries seems to be important and necessary, and the amount of metal pollutants and their entry sources into the aquatic environment and also their effects in different aquatic tissues should be continuously monitored. The actual effects of nanotechnology must be determined and identified before the appearance of nano-waste in the environment and the introduction of new nano-products to the market. Proper management of these new compounds can prevent

irreversible pollution and the consequences of the entry of toxic amounts because green plants and algae are the first chains of living in nature, the destruction of which destroys many living organisms in the continuity of the food chain.

GRANT SUPPORT DETAILS

The present research did not receive any financial support

CONFLICT OF INTEREST

The authors declare that there is not any conflict of interests regarding the publication of this manuscript. In addition, the ethical issues, including plagiarism, informed consent, misconduct, data fabrication and/ or falsification, double publication and/or submission, and redundancy has been completely observed by the authors.

LIFE SCIENCE REPORTING

No life science threat was practiced in this research.

REFERENCES

Abdelhameed, R. M., Abdel-Gawad, H. and Emam, H. E. (2021). Macroporous Cu-MOF@ cellulose acetate membrane serviceable in selective removal of dimethoate pesticide from wastewater. *J. Of. Env. Che. Eng*, *9*(2), 105121.

Aghoutane, Y., Diouf, A., Österlund, L., Bouchikhi, B. and El Bari, N. (2020). Development of a molecularly imprinted polymer electrochemical sensor and its application for sensitive detection and determination of malathion in olive fruits and oils. *Bio*, *132*, 107404.

Bacchetta, R., Santo, N., Marelli, M., Nosengo, G. and Tremolada, P. (2017). Chronic toxicity effects of ZnSO4 and ZnO nanoparticles in Daphnia magna. *Env. Res*, *152*, 128-140.

Bownik, A. (2017). Daphnia swimming behaviour as a biomarker in toxicity assessment: a review. *Sci. Of. The. Tot. Env*, *601*, 194-205.

Bozich, J., Hang, M., Hamers, R. and Klaper, R. (2017). Core chemistry influences the toxicity of multicomponent metal oxide nanomaterials, lithium nickel manganese cobalt oxide, and lithium cobalt oxide to Daphnia magna. *Env. Tox. And. Che*, *36*(9), 2493-2502.

Buchman, J. T., Bennett, E. A., Wang, C., Tamijani, A. A., Bennett, J. W., Hudson, B. G. and Haynes, C. L. (2020). Nickel enrichment of next-generation NMC nanomaterials alters material stability, causing unexpected dissolution behavior and observed toxicity to S. oneidensis MR-1 and D. magna. *Env. Sci. Nan*, *7*(2), 571-587.

Ch, P., and Jadhav, U. (2021). A Simple Colorimetric Detection of Malathion Using Peroxidase Like Activity of Fe3O4 Magnetic Nanoparticles. *ES. Foo. Agr*, *3*.

Chakrabarti, S. and Dutta, B. K. (2004). Photocatalytic degradation of model textile dyes in wastewater using ZnO as semiconductor catalyst. *J. Of. Haz. Mat*, *112*(3), 269-278.

Chingombe, P., Saha, B. and Wakeman, R. J. (2006). Sorption of atrazine on conventional and surface modified activated carbons. *J. Of. Col. And. Int. Sci*, *302*(2), 408-416.

Ehrampoosh, M. H., Moussavi S., Ghaneian, M. T., Rahimi, S. and Fallahzadeh, Z. H. (2010). Comparison between tubular and batch reactors in removal of methylene blue dye from simulated textile wastewater using TiO2/UV-C photocatalytic process. *J. Of. Yaz. Hea. Sun, 9(1)*, 1-9.

Gajda-Meissner, Z., Matyja, K., Brown, D. M., Hartl, M. G., and Fernandes, T. F. (2020). Importance of Surface Coating to Accumulation Dynamics and Acute Toxicity of Copper Nanomaterials and Dissolved Copper in Daphnia magna. *Env. tox. And. che*, *39*(2), 287-299.

Guo, Z., Ma, R., and Li, G. (2006). Degradation of phenol by nanomaterial TiO2 in wastewater. *Che. eng. J*, *119*(1), 55-59.

Hong, P. T. K., and Jang, C. H. (2020). Sensitive and label-free liquid crystal-based optical sensor for the detection of malathion. *Ana. bio*, *593*, 113589.

Jaafarzadeh, N., Ghanbari, F., and Ahmadi, M. (2017). Catalytic degradation of 2, 4-dichlorophenoxyacetic acid (2, 4-D) by nano-Fe2O3 activated peroxymonosulfate: influential factors and mechanism determination. *Chem*, *169*, 568-576.

Jafari, A. J., Kalantari, R. R., Gholami, M., and Esrafili, A. (2012). Photocatalytic removal of aniline from synthetic wastewater using ZnO nanoparticle under ultraviolet irradiation. *Ira. J. Of. Hea. And. Env*, *5*(2), 167-178.

Javid, A., Moghaddas, F., Yosefi, F., Davardoost, F. and Ghodrati, F. (2015). Comparing Efficiency of TiO2 Nano-Particles with TiO2 Nano-Fiber in Removing Reactive Blue 19 by Photo-Catalytic Oxidation Process. *J. Of. Hea*, *6*(3), 245-255.

Kassiri, H., Rabbani, D., Mohebi, F., Dehghani, R. and Takhtfiroozeh, S. (2021). A review on the removal methods of organophosphate insecticide malathion from the environment. *J. Of. Ent. Res*, *45*(1), 145-152.

Khan, K., Khan, P. M., Lavado, G., Valsecchi, C., Pasqualini, J., Baderna, D. and Benfenati, E. (2019b). QSAR modeling of Daphnia magna and fish toxicities of biocides using 2D descriptors. *Che*, *229*, 8-17.

Khan, P. M., Roy, K. and Benfenati, E. (2019a). Chemometric modeling of Daphnia magna toxicity of agrochemicals. *Che*, *224*, 470-479.

Lin, C. C., and Lee, C. Y. (2020). Adsorption of ciprofloxacin in water using Fe3O4 nanoparticles formed at low temperature and high reactant concentrations in a rotating packed bed with co-precipitation. *Mat. Che. And. Phy*, *240*, 122049.

Masudi, A., Jusoh, N. W. C., Jusoh, R., Jaafar, N. F., Jalil, A. A., Firdausi, A. and Hartanto, D. (2020). Equidistant crystal distortion arrangement of copper doped magnetite for paracetamol degradation and optimization with response surface methodology (RSM). *Materials Che. And. Phy*, *250*, 122995.

Mehdipour, M., Ansari, M., Pournamdari, M., Zeidabadinejad, L., and Kazemipour, M. (2020). Selective extraction of malathion from biological fluids by molecularly imprinted polymer coated on spinel ZnFe2O4 magnetic nanoparticles based on green synthesis. *Sep. Sci. And. Tec*, 1-11.

Nidheesh, P. V., Gandhimathi, R. and Ramesh, S. T. (2013). Degradation of dyes from aqueous solution by Fenton processes: a review. *Env. Sci. And. Pol. Res*, *20*(4), 2099-2132.

Nogueira, D. J., Vaz, V. P., Neto, O. S., da Silva, M. L. N., Simioni, C., Ouriques, L. C. and Matias, W. G. (2020). Crystalline phase-dependent toxicity of aluminum oxide nanoparticles toward Daphnia magna and ecological risk assessment. *Env. Res*, *182*, 108987.

Olaniran, A. O., Singh, L., Kumar, A., Mokoena, P., and Pillay, B. (2017). Aerobic degradation of 2, 4-dichlorophenoxyacetic acid and other chlorophenols by Pseudomonas strains indigenous to contaminated soil in South Africa: Growth kinetics and degradation pathway. *App. Bio. And. Mic*, *53*(2), 209-216.

Parastar, S., Poureshg, Y., Nasseri, S., Vosoughi, M., Golestanifar, H., Hemmati, S. and Asadi, A. (2012). Photocatalytic removal of nitrate from aqueous solutions by ZnO/UV process. *J. Of. Hea*, *3*(3), 54-61.

Prosposito, P., Burratti, L. and Venditti, I. (2020). Silver nanoparticles as colorimetric sensors for water pollutants. *Chem*, *8*(2), 26.

Qhasemi, Z., Yonsi, H. and Zinatizadeh, A. A. (2016). Efficiency of photo catalyst of titanium Nano oxide stabilized on Fe-ZSM-5 zeolite in removing organic pollutants from oil refinery wastewater. *Journal of Wat. And. Sew*, *27*(2), 22-33.

Sagir, M., Tahir, M. B., Akram, J., Tahir, M. S. and Waheed, U. (2021). Nanoparticles and Significance of Photocatalytic Nanoparticles in Wastewater Treatment: A Review. *Cur. Ana. Che*, *17*(1), 38-48.

Soares, O. S. G. P., Pereira, M. F. R., Órfão, J. J. M., Faria, J. L. and Silva, C. G. (2014). Photocatalytic nitrate reduction over Pd–Cu/TiO2. *Che. Eng. J*, *251*, 123-130.

Surendra, B., Raju, B. M., Onesimus, K. N. S., Choudhary, G. L., Paul, P. F. and Vangalapati, M. (2020). Synthesis and characterization of Ni doped TiO2 nanoparticles and its application for the degradation of malathion. *Materials Today: Pro*, *26*, 1091-1095.

Titus, D. and Samuel, E. J. J. (2019). Photocatalytic Degradation of Azo Dye Using Biogenic SnO 2 Nanoparticles with Antifungal Property: RSM Optimization and Kinetic Study. *J. Clu. Sci*, *30*(5), 1335-1345.

Yazdani, M., Bahrami, H. and Arami, M. (2014). Preparation and characterization of chitosan/feldspar biohybrid as an adsorbent: optimization of adsorption process via response surface modeling. *Sci. Wor. J*, 2014.

Zhang, F., Wang, Z., Song, L., Fang, H. and Wang, D. G. (2020). Aquatic toxicity of iron-oxide-doped microplastics to Chlorella pyrenoidosa and Daphnia magna. *Env. Pol*, *257*, 113451.

Zhou, N., Zhang, Y., Nian, S., Li, W., Li, J., Cao, W. and Wu, Z. (2017). Synthesis and characterization of Zn1-xCoxO green pigments with low content cobalt oxide. *J. All. Com*, *711*, 406-413.

Zhou, Y., Jiang, J., Gao, Y., Ma, J., Pang, S. Y., Li, J. and Yuan, L. P. (2015). Activation of peroxymonosulfate by benzoquinone: a novel nonradical oxidation process. *Env. sci. tec*, *49*(21), 12941-12950.

Zuo, H. G., Yang, H., Zhu, J. X., Guo, P., Shi, L., Zhan, C. R. and Ding, Y. (2019). Synthesis of Molecularly Imprinted Polymer on Surface of TiO 2 Nanowires and Assessment of Malathion and its Metabolite in Environmental Water. *J. of. Ana. Che*, *74*(10), 1039-1055.

Yao, Y., Cai, Y., Lu, F., Wei, F., Wang, X. and Wang, S. (2014). Magnetic recoverable MnFe2O4 and MnFe2O4-graphene hybrid as heterogeneous catalysts of peroxymonosulfate activation for efficient degradation of aqueous organic pollutants. *J. haz. mat*, *270*, 61-70.